G.F. Ferrazzano, T. Cantile, M. Coda, A. Ingenito

Department of Paediatric Dentistry, "Federico II" University of Naples, Naples, Italy

e-mail: marcocoda@fastwebnet.it

New approach in paediatric dentistry: ultrasonic nondestructive evaluation of restorative dental materials. Experimental study.

ABSTRACT

Aim *The ultrasonic inspection is a non invasive method which is very developed in the industrial field, for the non-destructive evaluation of materials, and in the medical field, for the ultrasound diagnostic analysis. In paediatric dentistry the most widely used non-destructive evaluation is the X-ray technique. Radiographs are valuable aids in the oral health care of infants, children, adolescents, allowing dentists to diagnose and treat oral diseases that cannot be detected during a visual clinical examination. The aim of this in vitro study was to analyse the ultrasonic non-destructive evaluation (UT-NDE) technique to inspect both dental materials internal structure and the form and position of internal defects in order to obtain a diagnostic method, free of ionising radiations, in paediatric dentistry. Moreover the ultrasonic inspection (UT) could be a rapid method of diagnosis in uncooperative paediatric patients.*

Materials and methods *Study design: Experimental samples were manufactured with the characteristics of a large composite or glass ionomer cement paediatric dental restoration, in terms of either size or operative technique used. Characteristics of the common restorations were analysed and reproduced* in vitro*, using the same operative conditions, also adding operative defects into some samples. All the samples were subjected to an innovative UT test using the pulse echo immersion scanning technique. Both C-scans and full volume scans were carried out during the experimental programme. To enhance the data obtained from the UT scan, a digital system (Ecus Inspection software) for signal detection, archiving, processing and displaying was used.*

Results *UT images showed the presence of internal defects in the dental materials. It was also possible to inspect very thin discontinuity such as the one represented by the fluid resin. Statistics: In order to execute the statistical analysis, the values of electric voltage measured in five higher white points and in five higher grey points of the pictures pixels, were measured for each sample. Then, the average values and the standardised data were calculated.*

Conclusion *In conclusion, the ultrasonic test could be a diagnostic non-invasive method in paediatric patients, capable to evaluate the quality of the restorative teeth filling, showing internal little defects.* In vivo *application of this diagnostic method should be developed.*

Keywords *Caries; Dental diagnosis; Dental restoration; Ultrasounds.*

Introduction

The *in vitro* evaluation of dental restoration materials through a non-invasive analysis method, that does not require the use of x-rays, or the destruction of the sample, is an important objective in clinical dentistry [Asmussen and Munksgaard, 1985]. In the clinical practice, paediatric dentists do not have many diagnostic tools to evaluate the quality of a dental restoration. In fact, the only significant non-destructive evaluation that could help physicians about the integrity of a dental restoration is the x-ray test, which has some important limits: the image obtained through x-ray methods is bi-dimensional, and for this reason it is not possible to establish exactly the position of defects; moreover, this evaluation method has not enough resolution to show small defects or fine details. In fact, it was shown that traditional or digital dental x-ray cannot detect early enamel lesions on proximal surfaces with a high accuracy [Wakoh and Kuroyanagi, 2001]. Moreover, another study assessed that conventional or digital photostimulable phosphor (PSP) x-ray techniques were less accurate, with more ionising radiations, respect to other new radiographic methods, as Cone Beam Computed Tomography (CBCT), in detecting small (0.2 mm) mesio-distal root perforations and other endodontic lesions or features [Shokri et al., 2015].

Finally, x-ray is a diagnostic method that needs the cooperation of paediatric patients and certainly, cannot inspect the adhesive interface, made of fluid resin, characterised by a thickness of few microns [John, 2006]. Besides, the non-invasive nature of x-rays is dependent on the absorbed dose; the use of a method that has not noxious effects on the organism, such as the ultrasonic method, is a very interesting goal for the research activities in paediatric dentistry. For this reason, ultrasonic test (UT) of the tooth has been suggested as an alternative method for identifying dental pathology [John, 2006; Sun et al., 2008].

The ultrasonic inspection is a non invasive method which is very developed in the industrial field, for the non-destructive evaluation of materials, and in the medical field, for the ultrasonic diagnostic analysis. Especially in the medical field, the non invasive nature of ultrasonic waves is the ideal method for clinical diagnostics. In the industrial field, subsurface defects are easily identified when an ultrasonic beam has been directed perpendicular to the surface. Because the time of flight (travel time) of the sound waves will be different in two different mediums, it is possible in dental diagnosis to differentiate between sound and demineralised enamel. Sonic waves that are reflected back (echoes) toward the transducer cause a change in the thickness of the piezoelectric crystal, which in turn produces an electrical signal that can be amplified, processed and ultimately digitally stored [Schwalbe et al., 1999; Achenbach, 2002; Hosten et al., 2002; Hrovatin et al., 2006].

Yanikoglu et al. [2000] studied caries using a transducer and Novascope 4500 thickness gauge (NDT Systems, Waltham, MA, USA) that automatically reported thickness measurements. The study reported 88% sensitivity and 86% specificity in comparison to histology and bite-wing radiographs.

Another study analysed caries disease in approximal surfaces using an ultrasonic caries detector (UCD) [Matalon et al., 2007]. The study reported a sensitivity of 0.82 compared with 0.75 for bite-wing radiographs and specificity was 0.75 versus 0.9 for radiographs.

A study based on using a finite-element (FE) model, analysed tooth phantoms reflecting actual tooth anatomy with various defects [Ghorayeb et al., 1998]. The results showed the finite element code's ability to predict and visualise ultrasonic wave propagation in complexes dental structures.

Recently, a study analysed the reliability of ultrasound imaging coupled with colour power doppler for monitoring the healing after nonsurgical endodontic therapy [Maity et al., 2011]. Results show that ultrasounds with color power doppler is an efficient tool for monitoring bone healing as compared to the conventionally employed radiographic method.

The aim of this *in vitro* study is to verify the capability of the ultrasonic technique to: 1) inspect the quality of the adhesive interface between restoration and tooth surface; 2) verify the innermost continuity among the layers of filling material polymerised at different times; 3) detect the internal defects of the filling material manually compacted by the operator (porosities, voids, etc.); 4) analyse the adhesive layer between different filling materials; 5) examine the presence of artificial internal defects having known dimensions and shapes.

Materials and methods

Fourteen samples were manufactured with the characteristics of a large dental restoration, in terms of either size or operative technique used. The manufacture of the samples was carried out at the "Federico II" University of Naples, Department of Paediatric Dentistry, Naples, Italy. The sample shape was cylindrical with diameter of 10 mm and height of 6 mm and was produced using teflon moulds (Fig. 1).

The materials used to manufacture the samples were introduced into the mould hole making just one or two layers; common paediatric dental restoration materials were used: solid composite (Charisma©, Heraeus Kulzer GmbH, South Bend, IN, USA), high viscosity glass ionomer cement (GC Equia©, GC EUROPE, Leuven, Belgium) and adhesive resin (Prime & Bond NT©, Dentsply International, York, PA, USA); for the samples having two layers, polymerisation occurred one layer at a time. A clear polyester film was laid under the first layer as well as on the second layer during the polymerisation phase to obtain the smoothest possible surface on the sample bases (required to carry out an efficient UT NDE). The polymerisation time used for each of the layers was the one indicated by the manufacturer of the examined material; materials polymerisation was obtained using

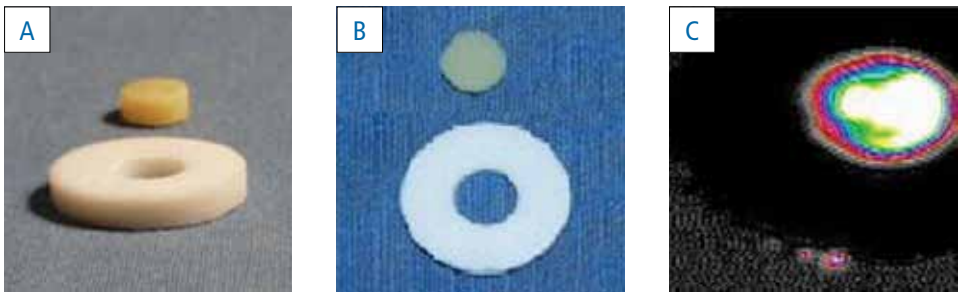

FIG. 1 Image of a sample of dental composite material with the teflon mould used to build the samples.
A side view of sample 1.
B view from above of sample 1.
C C-scan of sample 1 made of 1 layer of dental composite material.

Sample id	Composition	Artificial Defect	C-scan	Full volume scan
1	1 layer of dental composite material (Charisma-Kulzer)	-	Yes	No
2	2 layers of dental composite material (Charisma-Kulzer) with interposition of adhesive resin	-	Yes	Yes
3	2 layers of dental composite material (Charisma-Kulzer) without interposition of adhesive resin	-	Yes	Yes
4	1 layer of glass ionomer cement (GC Equia) and 1 layer of dental composite material (Charisma-Kulzer) without interposition of adhesive resin	-	Yes	No
5	2 layers of glass ionomer cement (GC Equia)	0.6 mm central hole, filled by liquid resin	No	Yes
6	2 layers of glass ionomer cement (GC Equia)	0.4 mm copper wire	Yes	Yes
7	2 layers of glass ionomer cement (GC Equia)	0.7 mm iron wire	No	Yes
8	2 layers of dental composite material (Charisma-Kulzer) without interposition of adhesive resin	0.2 mm nylon bristle	No	Yes
9	2 layers of glass ionomer cement (GC Equia)	0.5 mm nylon bristle	Yes	Yes
10	1 layer of glass ionomer cement (GC Equia) polymerised at one time	0.8 mm diameter cotton pad	Yes	Yes
11	2 layers of glass ionomer cement (GC Equia)	0.8 mm diameter cotton pad	Yes	Yes
12	2 layers of glass ionomer cement (GC Equia)	1 mm diameter poly-styrene sphere	Yes	Yes
13	1 layer of glass ionomer cement (GC Equia) polymerised at one time	1.5 mm diameter quartz sphere	No	Yes
14	2 layers of glass ionomer cement (GC Equia)	1.5 mm diameter quartz sphere	No	Yes

TABLE 1 Samples subjected to UT NDE.

LED Curing Light (Elipar™, 3M Italy S.p.a., Pioltello, Italy). As described in Table 1, the samples subjected to UT NDE were made as follows.

- Sample n. 1: One layer of dental composite material (Charisma-Kulzer).
- Sample n. 2: Two layers of dental composite material (Charisma-Kulzer) with interposition of adhesive resin.
- Sample n. 3: Two layers of dental composite material (Charisma-Kulzer) without interposition of adhesive resin.
- Sample n. 4: One layer of glass ionomer cement (GC Equia) and one layer of dental composite material (Charisma-Kulzer) without interposition of adhesive resin.
- Sample n. 5: Two layers of glass ionomer cement (GC Equia), but before polymerisation of the two layers, a central hole of 0.6 mm was made, filled by liquid resin.
- Sample n. 6: Two layers of glass ionomer cement (GC Equia), with interposition, before polymerisation, of 0.4 mm Ø of a cylindrical copper wire.
- Sample n. 7: Two layers of glass ionomer cement (GC Equia) with interposition, before polymerisation, of a cylindrical iron wire of 0.7 mm Ø.
- Sample n. 8: Two layers of dental composite material (Charisma-Kulzer) without adhesive resin, but with interposition of 0.2 mm Ø of a nylon bristle.
- Sample n. 9: Two layers of glass ionomer cement (GC Equia) with interposition of adhesive resin and 0.2 mm Ø of a cylindrical nylon bristle.
- Sample n. 10: one layer of glass ionomer cement (GC Equia) polymerised at one time with interposition of a cotton pad of 0.8 mm, before polymerisation.
- Sample n. 11: Two layers of glass ionomer cement (GC Equia), with interposition of a cotton pad of 0.8 mm, before polymerisation.
- Sample n. 12: Two layers of glass ionomer cement (GC Equia), with interposition of 1 mm Ø of a polystyrene sphere, before polymerisation.
- Sample n. 13: One layer of glass ionomer cement (GC Equia) polymerised at one time, with interposition of 1.5 mm Ø of a quartz sphere, before polymerisation;
- Sample n. 14: Two layers of glass ionomer cement (GC Equia), with interposition of 1.5 mm Ø of a quartz sphere, before polymerisation.

The samples were examined through UT NDE at the LAPT, Dept. of Materials and Production Engineering, "Federico II" University of Naples, Italy. The new experimental ultrasonic system was composed of a

transducer (probe) (Harisonic, Staveley, NDT, WA, USA) and a thickness gauge (NDT, Novascope, 4500, Waltham, MA, USA) connected to a computerised system that stored and analysed data. The contact transducer was an immersion-type, with a 6 mm diameter tip contact, 25 MHz nominal center frequency. The probe was oriented perpendicular to the surface during the contact with each sample to get the echo signals as calibrated before. Because of their small size, the samples were immersed in the water tank mounted in their teflon mould.

Test results, which are documented by imaging methods, are repeatable, describing the tested area and allow an easy separation of geometry indication from real defect indications. In fact, in laboratory work, during development and optimisation of test procedures, the imaging technique (e.g. via A-scan, B-scan or C-scan) is helpful, since possible additional or unexpected effects are better recognised and interpreted. However, as this technique of ultrasonic analysis is still at an experimental stage, only low resolution ecographic images could be obtained. A-scan means that a short impulse is generated into the object (sample) and echoes are displayed as function of time (depth). B-scan means that, if the A-scan concept is combined with movement of the probe along the surface, a B-scan is the result: it depicts the acoustical side projection of the object. Meanwhile, via C-scan are recorded echo amplitudes in relation to probe position: it depicts the object top view of amplitude.

In this study the samples were subjected to UT test using the pulse echo immersion scanning technique [Goracci et al., 1993] and the waves made by the A-scan were entirely considered, analysing front echo, back (bottom) echo and middle echo.

During the pulse echo test, the waves that impacted on the frontal surface of the sample, produced the so called front echoes; the waves that reflect on the end of the thickness of the sample produced the back (bottom) echoes. And if in the sample are included defects or gaps, the waves reflect on theme, producing the middle echoes, that describes the presence of above mentioned defects and also their position in the thickness, depending on the delay time respect to front echo.

The UT NDE software used, is based on the acquisition of the entire UT waves. This type of scanning technique is defined as full volume scanning and consists in the automatic acquisition of the digitised UT waveform for each material interrogation point during a plane X-Y scan with a predefined step. The UT waveforms are then organised in a full volume database, providing information on any thickness portion of the material under examination. It consists in a collection of single files, each containing one UT waveform. The availability of a full volume UT database allows for a number of procedures useful for UT NDE such as 2D UT image generation and processing, UT waveform retrieval, display and processing, etc.

Both C-scans [Teti, 1987] and full volume scans [Teti and Buonadonna, 1998] were carried out during the experimental programme (Table 1).

As above mentioned, to enhance the data obtained from the UT scans, a digital system for signal detection, archiving, processing and displaying was used. Two software were developed to carry out this data enhancing procedure from the Dept. of Materials and Production Engineering: P wave (Matlab software – MathWorks Inc., Natick, MA, USA) and Ecus Inspection (Labview software, National Instruments Corporation, Austin, TX, USA).

In order to execute the statistical analysis, the values of electric voltage measured in five higher white points and in five higher grey points of the pictures of seven samples (Samples 1-2-6-7-10-12-14), were measured. This operation was conducted using the "Ecus Inspection" software. Then, the average values and the standardised data were calculated, as reported in table 2.

		Original Data					Average	SD	Standardized Data				
Sample 1 One Layer	White	1,81	1,94	1,97	1,87	1,95	1,53	0,400106	0,6948	1,0197	1,0947	0,8448	1,0447
	Gray	1,13	1,16	1,23	1,1	1,16			-1,0047	-0,9298	-0,7548	-1,0797	-0,9298
Sample 2 Two Layers	White	1,74	1,64	1,7	1,67	1,65	1,55	0,152319	1,2671	0,6106	1,0045	0,8075	0,6762
	Gray	1,4	1,33	1,54	1,37	1,43			-0,9651	-1,4246	-0,046	-1,162	-0,7681
Sample 7 Iron	White	1,6	1,74	1,47	1,57	1,67	1,17	0,471306	0,9166	1,2137	0,6408	0,8529	1,0651
	Gray	0,75	0,73	0,76	0,7	0,69			-0,8869	-0,9293	-0,8657	-0,993	-1,0142
Sample 10 Cotton	White	2,14	2,11	2,11	2,21	2,18	1,35	0,844748	0,9352	0,8997	0,8997	1,0181	0,9825
	Gray	0,49	0,52	0,62	0,61	0,51			-1,0181	-0,9825	-0,8642	-0,876	-0,9944
Sample 6 Copper	White	1,7	1,97	1,67	1,84	1,81	1,33	0,507088	0,7375	1,27	0,6784	1,0136	0,9545
	Gray	0,79	0,83	1	0,85	0,8			-1,057	-0,9781	-0,6429	-0,9387	-1,0373
Sample 12 Polystirene	White	1,23	1,16	1,13	1,06	1,1	0,67	0,489698	1,1354	0,9924	0,9312	0,7882	0,8699
	Gray	0,22	0,19	0,25	0,15	0,25			-0,9271	-0,9884	-0,8658	-1,07	-0,8658
Sample 14 Quartz	White	-1,1	-1,13	-1,08	-1,15	-1,11	-1,57	0,484609	0,976	0,9141	1,0173	0,8729	0,9554
	Gray	-2,01	-2,06	-2,04	-1,99	-2,06			-0,9018	-1,0049	-0,9637	-0,8605	-1,0049

TABLE 2 Values of electric voltage standardized using the Ecus Inspection software.

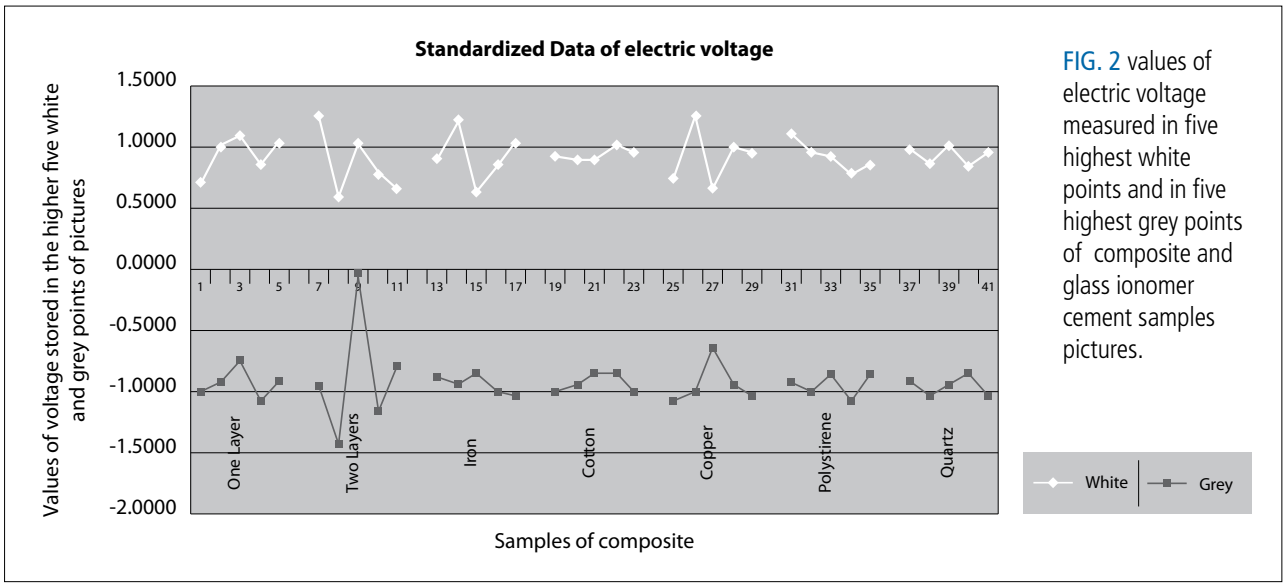

FIG. 2 values of electric voltage measured in five highest white points and in five highest grey points of composite and glass ionomer cement samples pictures.

MANOVA	Dev	Dev/gl	QMA/QME	
	gl	Sq	QM	F	P value
White/Gray	1	14,12	14,12105	3243,024	2,91E-51
Sample	6	74,29756	12,38293	2843,848	1,12E-67
Interaction	6	2,29	0,382055	87,74224	1,19E-26
Error	56	0,24	0,004354		
	69	90,95			

TABLE 3 MANOVA data results.

A graphic representation of these data was obtained using a spreadsheet software (Fig. 2).

The analysed data referred to the experimental work conducted having as bases two factors: the first one considered only two levels (white and gray shades of the scan-point), and the second one considered several levels (type of sample and type of defect: one layer, two layers, iron, cotton, copper, polystyrene, quartz).

For the characteristics of the research, the analyst was interested in assessing the presence of a significant statistical importance of the first factor; in order to answer to this question, the Manova analysis was used, which allowed to show both the possible significant importance of the second factor and the interaction between the two factors. The data stored during the Manova analysis are shown in Table 3.

Results

The results were evaluated examining the reflected wave stored during the scanning of the samples. For the C-scan, such as for the A-scan, the images derived from the computing enhancement were considered.

Some C-scan images are composed of 16 colours, while some other of 256 tonalities of grey. The colours or the grey-scale are used from the software to indicate discontinuity or compactness of the material with the aim of giving the ultrasound image of the sample examined, just like the image of B-scan used in medical field for diagnostic procedures. In figure 1-3-4-5-6-7 are shown the resulted UT scans of samples.

Several interesting results were shown by C-Scan of samples. In figure 1C, it was possible to notice the presence of two small defect areas on the edge of the sample represented by two green areas on the upper edge and the lower left corner of the sample. No defect was visible in the centre of the sample. The Teflon mould is visible in the image as a dark ring around the sample.

Figure 3A reported the UT image from the C-scan of sample 6, where it was possible to identify the copper wire which appears as a horizontal dark/red stripe on a green spotted/white background. A similar oblique dark red stripe in the upper right corner of the image can be correlated with lack of adhesion between the two

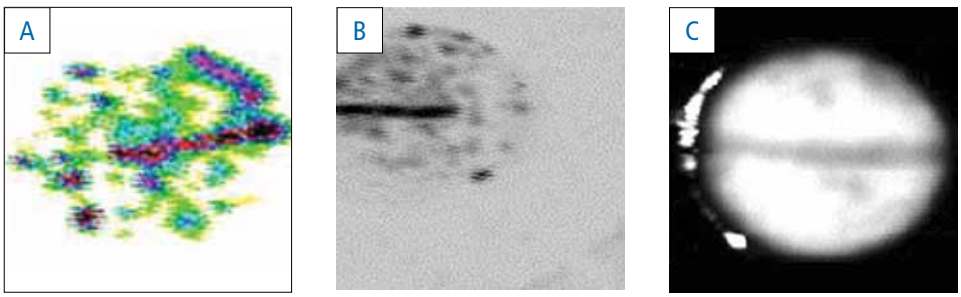

FIG. 3 A C-scan of sample 6 made of 2 layers of dental glass ionomer cement with inclusion of a copper wire. B C-scan of sample 6 after image enhancement. C C-scan of sample 6 obtained through the Ecus Inspection software.

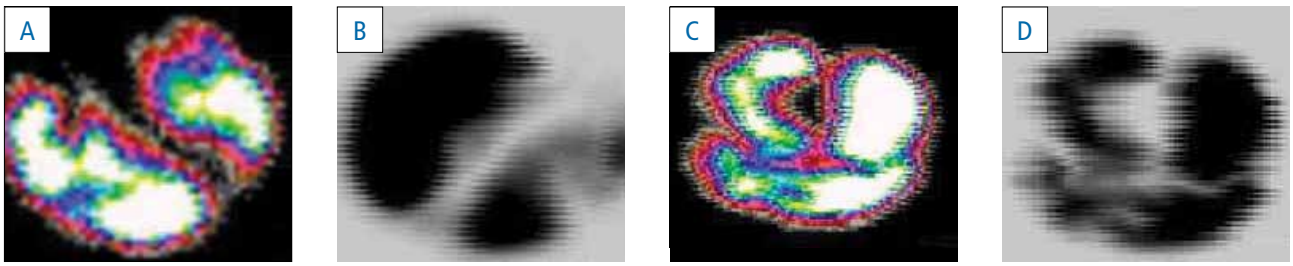

FIG. 4 A C-scan of sample 9 made of 2 layers of dental glass ionomer cement with inclusion of a 0.5 mm thick nylon bristle. B C-scan of sample 9 after image enhancement. C C-scan of sample 12 made of 2 layers of dental glass ionomer cement with inclusion of a 1 mm diameter polystyrene sphere. D C-scan of sample 12 after image enhancement.

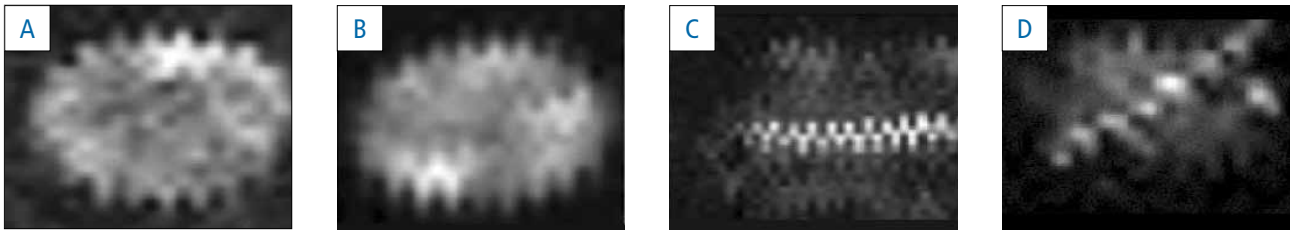

FIG. 5 Full volume scanning images. A image of sample 2 made of two layers with interposition of fluid resin: image obtained with time gate on back echo. B Image of sample 3 made of two layers without interposition of fluid resin. C Full volume scanning of sample 6. D Full volume scanning of sample 6 with a different angle of inspection.

glass ionomer cements (GC Equia) layers which include the copper wire. This defect appeared in the UT image because the time gate used allowed the identification of all defects in the material thickness comprised in that time gate. In figure 3B, the UT image from the C-scan of sample 6 was reported after application of an image enhancement procedure. The light grey ring around the sample is the teflon mould displaying a UT response different from the sample material. The horizontal dark stripe, representing the copper wire, was more evident than in Figure 3-A. Some dark zones are also visible, due to lack of adhesion between the two layers of glass ionomer cement (GC Equia). In Figure 3-C, the copper wire was in this case particularly evident as a horizontal dark stripe. Some dark spots in the rest of the material image may confirm lack of adhesion between the two glass ionomer cement layers shown in figure 3B.

In figure 4A, reporting the UT image from the C-scan of sample 9, it was possible to identify the nylon bristle which appeared as an oblique dark stripe. It was possible to notice that the extremity of the dark stripe in the upper left corner was larger than the one on the opposite side. This may be due to the bad adaptation of the glass ionomer cement (GC Equia) around the nylon bristle in that zone. Figure 4B showed the UT image from the C-scan of sample 9 after application of an image enhancement procedure; that procedure made evident the zones of good adhesion (black) and the zones of bad adhesion (white).

In figures 4C and 4D, the UT images from the C-scan of sample 12, showed in the centre of the image the polystyrene sphere, represented by a dark spot. Besides, zones of lack of adhesion between the two layers of glass ionomer cement were evident on the upper edge and on the left edge of the sample image. The white spots are the zones where the material had no internal defects.

Also Full Volume Scanning of samples showed interesting images.

In figure 5A, the image from the full volume scanning of sample 2 showed the dark areas on the upper edge and in the centre of the sample image; this indicated a lack of adhesion between the two layers of composite material.

Figure 5B represented the image from the full volume scanning of sample 3. An unpredictable result was given by this test. In fact in this sample there was no interposition of fluid resin, but the UT evaluation has shown the presence of a discontinuity between the layers polymerised in two phases (the discontinuity is showed by the grey areas in the image).

Figures 5C and 5D show the images obtained from the full volume scanning of sample 6. These images were obtained by using P-wave software.

The copper wire was represented by a bright horizontal stripe in figure 5C and by a bright oblique stripe in figure 5D. Two small dark stripes next to the extremities of the copper wire were also visible, which may represent a low adaptation of the glass ionomer cement around the artificial defect.

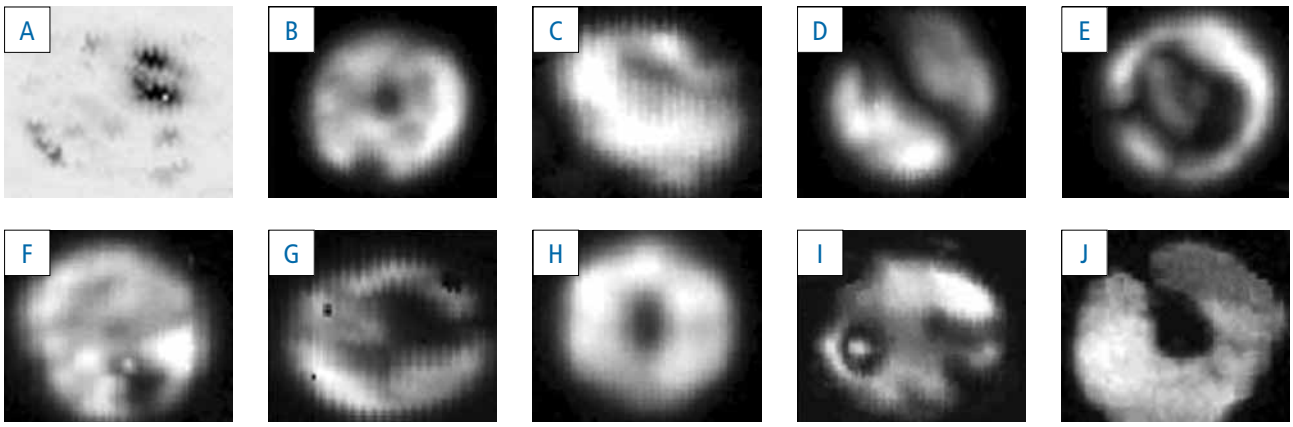

FIG. 6 Full volume scanning of samples obtained through Ecus Inspection software. A Sample 12 made of 2 layers of dental glass ionomer cement with inclusion of a 1 mm diameter polystyrene sphere. B Sample 5 made of two layers of dental glass ionomer cement with a central hole of 0.6 mm filled of fluid resin. C Sample 8 made of two layers of GIC with inclusion of a 0.2 mm nylon bristle. D Sample 9 made of two layers of GIC with inclusion of a 0.5 mm nylon bristle. E Sample 10 made of two layers of GIC with inclusion of a 0.8 mm cotton pellet. F Sample having the same characteristics of sample 10 but with a better compression of glass ionomer cement. G Sample 12 made of two layers of GIC with inclusion of a 1 mm polystyrene sphere: image obtained with time gate on back echo through P-wave software. H Sample having the same characteristics of sample 12 but with a better compression of glass ionomer cement: image obtained with time gate on back echo through P-wave software. I Sample 13 made of one layer of GIC with inclusion of a 1.5 mm quartz sphere. J Sample 14 made of two layers with inclusion of a 1.5 mm quartz sphere.

In figure 6 the images from the full volume scan of all the other samples were reported. In figure 6A the defect zone was represented from a very evident dark spot that indicates the presence of the polystyrene sphere.

In figure 6-B the image from the full volume scanning of sample 5 through a powerful scanning software (Ecus Inspection) was reported. The dark spot, which was given by the central hole filled by fluid resin, showed still better the discontinuity created by adhesive, as shown through the scan of sample 2.

Figure 6-E represented the Full volume scanning through Ecus software of sample 10, made of two layers with inclusion of a 0.8 mm cotton pad. The image resulting showed a great defect of adhesion all around the pad. Another type of construction of sample 10 was adopted successively; the second layer was not simply posed on the defect, but it was compressed on it. The image obtained from the scanning of this sample was reported in figure 6F. The defect area was restricted only to the pad contact area between the cotton pad and the layer of resin. The same result was given by two different kind of fabrication of sample 12 as shown in figures 6G and 6H. The softness of polystyrene sphere made it comparable to the cotton.

Figure 6I showed the full volume scanning of sample 13 made of one layer of glass ionomer cement with inclusion of a quartz sphere. The sphere was very evident as a white spot on the left side of the sample.

If sample 13 was fabricated in two layers, as made with sample 14, the quartz sphere had no way to move on the back of the sample. In fact it was visible as a black spot in figure 6J. In that image was also very evident the flowing of glass ionomer cement that included the quartz sphere leaving a bad adhesion zone on the upper left corner of the sample.

The scanning of sample 6, reported in figure 7A, showed that the copper wire was well evident along almost all its length. Through the multi-image function of the Ecus software (Fig. 7B), that allowed to see several very thick layers such as a tomography, it was possible to see that the copper wire was laying on an oblique plain, that was on several layers.

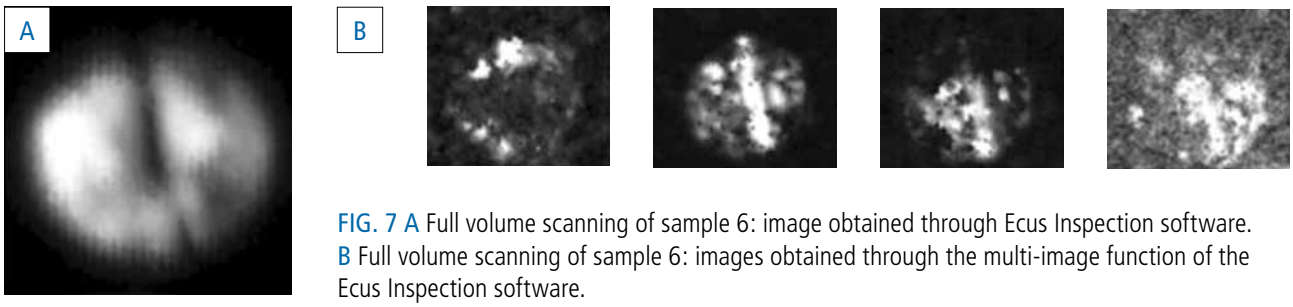

FIG. 7 A Full volume scanning of sample 6: image obtained through Ecus Inspection software. B Full volume scanning of sample 6: images obtained through the multi-image function of the Ecus Inspection software.

Discussion

The resulting data of Manova test showed an effective significant statistical importance of both factors and their interaction. The p-values resulted very low and the calculated F-values resulted greater of the F-values tabulated in relationship to the specific freedom degrees placed as numerator and denominator.

These tests conducted on the samples showed the validity of the ultrasonic scanning to evaluate the presence of internal defects inside resin composite and glass ionomer cement (GC Equia). It was possible to inspect also very thin discontinuity such as the one represented by the fluid resin.

Our results showed that the combination of techniques for signal data processing and results displaying, based on digital signals, yielded results capable to exploit the potential of ultrasonic inspection up to the limiting factors represented by the transducer and the low resolution of echo images.

Conclusion

In conclusion, the ultrasonic test could be a diagnostic method capable to evaluate the quality of the resin composite and glass ionomer cement teeth restorations, showing internal thickness and defects. The *in vivo* application of this diagnostic method should be developed to improve the scanning of objects with complex geometry, as the dental structures. Further studies are still necessaries to use this ultrasonic method in the diagnosis of dental diseases, particularly in paediatric cooperative and uncooperative patients.

References

- Asmussen E, Munksgaard EC. Adhesion of restorative resins to dentinal tissue, in posterior composite resin dental restorative materials. Vanherle & Smith editors, Utrecht, The Netherlands. P Szulc Publishing 1985;217-229.
- Wakoh M, Kuroyanagi K. Digital imaging modalities for dental practice. Bull Tokyo Dent Coll 2001 Feb;42(1):1-14. Review.
- Shokri A, Eskandarloo A, Noruzi-Gangachin M, Khajeh S. Detection of root perforations using conventional and digital intraoral radiography, multidetector computed tomography and cone beam computed tomography. Restor Dent Endod 2015 Feb; 40(1): 58–67.
- John C. Lateral distribution of ultrasound velocity in horizontal layers of human teeth. J Acoust Soc Amer 2006;119:1214–1226.
- Sun X, Witzel EA, Bian H, Kang S. 3-D finite element simulation for ultrasonic propagation in tooth. J Dent 2008;36(7):546-53.
- Schwalbe HJ, Bamfaste G, Franke RP. Non-destructive and non-invasive observation of friction and wear of human joints and of fracture initiation by acoustic emission. Proc Inst Mech Eng [H] 1999;213(1):41-8.
- Achenbach JD. Modeling for quantitative non-destructive evaluation. Ultrasonics 2002;40:1-10.
- Hosten B, Bacon C, Guilliorit E. Acoustic wave generation by microwaves and applications to non-destructive evaluation. Ultrasonics 2002;40(1-8):419-26.
- Hrovatin R, Petkovsek R, Diaci J, Mozina J. The applicability of a material-treatment laser pulse in non-destructive evaluations. Ultrasonics 2006;44 Suppl 1:1199-202.
- Yanikoglu FC, Ozturk F, Hayran O, Analoui M and Stookey GK. Detection of natural white spot caries lesions by an ultrasonic system. Caries Res 2000;34:225–232.
- Matalon S, Feuerstein O, Calderon S, Mittleman A, Kaffe I. Detection of cavitated carious lesions in approximal tooth surfaces by ultrasonic caries detector. Oral Surg Oral Med Oral Pathol Oral Radiol Endod 2007;103(1):109-13.
- Ghorayeb SR, Xue T, Lord W. A Finite Element study of ultrasonic wave propagation in a tooth phantom. J Dent Res 1998;77(1):39-49.
- Maity I, Kumari A, Shukla AK, Usha H, Naveen D. Monitoring of healing by ultrasound with color power doppler after root canal treatment of maxillary anterior teeth with periapical lesions. J Conserv Dent 2011;14(3):252-7.
- Teti R. Ultrasonic inspection of composite materials. In: Journées sur le controle qualité des matériaux composites;1987, Bordeaux 12–13 May: 205-219.
- Teti R, Buonadonna, P. Full volume ultrasonic NDE of CFRP Laminates. In: 8th European Conference on composites materials (ECCM-8);1998,Naples 1-5 June; Vol. 3:317-324.